Supplementary Materials:

Materials and Methods

Cell Culture

Please see table s1 for information regarding cell lines evaluated in this study. All cells were grown using standard cell culture techniques at 37 ˚C under 5% CO_2 and 15% O_2. UWB1.289 cells were cultured in a 1:1 solution of RPMI 1640:MEGM with bullet kit (Lonza, MEGM bullet kit:CC-3150) without gentamycin, plus 10% FBS and 1% penicillin/streptomycin (PS). UWB1.289-*BRCA1* restored cells were cultured in identical media with gentamycin at 200 µg/mL (ATCC recommended) for selection of the UWB1.289-*BRCA1* restored cells. UWB1.289 *PARP1* KO cell lines contained a puromycin resistance gene for selection and were cultured in media identical to UWB1.289 with puromycin at a concentration of 2 µg/mL. OVCAR8 *PARP1* KO cells also contained a puromycin resistance gene for selection and were cultured in RPMI 1640 with 10% FBS and 1% PS plus puromycin at a concentration of 2 µg/mL. All other cells were cultured in RPMI 1640 plus 10% FBS and 1% PS.

CRISPR/Cas9 mediated *PARP1* deletion in UWB1.289 and OVCAR8 EOC cell lines

CRISPR single guide RNA's (sgRNA) were designed to target the DNA binding domain of PARP-1, specifically Zinc Finger 1 which is essential to DNA binding and allosteric regulation of catalytic activity. Frameshift deletions in this region would result in early termination of protein synthesis, or a destabilized and non-functional protein. See guide sequences below.

Base pairs 178 – 197 – CGAGTCGAGTACGCCAAGAG**CGG**

Base pairs 179 – 198 – GAGTCGAGTACGCCAAGAGC**GGG**

Base pairs 234 – 253 – CCCCAAGGACTCGCTCCGGA**TGG**

The first exon of *PARP1* encodes Zinc Finger 1 amino acids 2 – 40 with the following nucleotide sequence. The three CRISPR sgRNA's used in this study targeted regions highlighted in yellow, green, or red lettering.

CGGTGGCCGGTGCGGCGTGTTCGGTGGCGGCTCTGGCCGCTCAGGCGCCTGCGGCTG GGTGAGCGCACGCGAGGCGGCGAGGCGGCAGCGTGTTTCTAGGTCGTGGCGTCGGGCTTCCG GAGCTTTGGCGGCAGCTAGGGGAGGATGGCGGAGTCTTCGGATAAGCTCTATCGAGTCGAGTA CGCCAAGAGCGGGCGCGCCTCTTGCAAGAAATGCAGCGAGAGCATCCCCAAGGACTCGCTCCG GATGGCCATCATGGTGCAGG

Next, sgRNA's were propagated by standard methods using stabl 3 E. Coli and DNA was harvested by mini-prep as previously described.

Lentivirus production and transfection

Using HEK-293T cells lentivirus was produced using 3 self-deactivating packaging plasmids (pMD2.g(VSVG), pRSV-REV, PMDLg/pRRE, Addgene). Packaging vectors were added to cells along with target plasmids and LipoD293 transfection reagent. The media was changed 24 hrs later and 48 hrs post transfection the medium supernatant was collected and stored at 4 ˚C overnight. Virus collection was repeated again 24 hrs after the initial collection. First, UWB1.289 and OVCAR8 cells were transfected with lentivrus containing Cas9 (lenti-Cas9-Blast, Addgene) for stable expression. Blastacidin (8 µg/mL) was used to select polyclonal populations of stable Cas9 expressing cells. Next, polyclonal Cas9 expressing UWB1.289 and OVCAR8 cell lines were transfected with lentivirus containing one of the three unique sgRNA to mediate *PARP1* deletion with puromycin resistance. *PARP1* KO polyclonal populations were then continuously selected under puromycin (2 µg/mL). Cas9 expression and *PARP1* deletion were confirmed by immunofluorescence (figure s1a) and Western blot protein analysis (figure s1b). Furthermore, PARP-2 and PARP-3 expression was examined by Western blot (figure s1b) to evaluate off-target effects of the sgRNA's used despite low probability of

such interactions as determined by sequence homology combined with protospacer adjacent motif (PAM) recognition.

Western blot and immunofluorescence analysis

To characterize the *PARP1* KO cell lines we used Western blot and immunofluorescent microscopy. These two methods were also used to compare DNA damage by measuring γH2AX in *PARP1* KO and parent cells treated with olaparib vs. DMSO controls.

Cell lysates for Western blot analysis were prepared by harvesting cells grown in 10 cm dishes that were 80% confluent. Cells were lysed in RIPA buffer with preservatives at 4 °C for 20 minutes and then sonicated. Samples were centrifuged at 15 G for 20 minutes at 4 °C. The supernatant was collected and protein was quantified using BioRad DC protein quantification assay. All samples were then diluted to a final concentration of 2 µg/µL and 1x laemmli buffer. Gel electrophoresis was performed using BioRad TGX pre-packed gels at 150 V for 1 hr. Gels were transferred to a PDVF membrane using BioRad turbo transfer at 1.3 A for 7 minutes. Membranes were blocked in Odyssey blocking buffer (LiCOR) for 1 hr. Anti-PARP-1 (1:1000) (PARP 46D11 Rabbit mAb, Cell Signaling Technologies), anti-Cas9 (1:800) (A-9000-050, Epigentek), anti-PARP2 (1:500) (4G8, Enzo), anti-PARP3 (1:500) (ALX-210-971, Enzo), anti-phoso-H2AX (1:5000) (anti-phospho-H2AX, Ser139, Millipore) or anti-Histone H3 (1:1000) (Histone H3 Antibody #9715, Cell Signaling Technologies) were then incubated with membranes overnight at 4° C. Next, membranes were washed 4 times in PBS w/ 0.2% tween 20 and fluorescent secondary antibodies (Thermo Fisher Scientific) were incubated for 1 hr in Odyssey Blocking buffer, 0.2% tween 20 and 0.1% SDS.

Cell microscopy analyzing PARP-1 and γH2AX was performed by plating cells in 24 well plates with cover slips. Cells were then fixed with 2% PFA and permeabilized using 0.5% Triton X. PARP-1 (1:1000) and γH2AX (1:5000) were stained using the same antibodies listed above. Immunofluorescence was performed with and without olaparib treatment. Olaparib exposure was

assayed at a single time point of 24 hrs. Olaparib treated cells stained for γH2AX were normalized to untreated controls and the difference was noted when significant (figure 1d).

Radiosynthesis of [^{125}I]KX1 and [^{18}F]FTT

1-(4-(Iodo-^{125}*I*)phenyl)-8,9-dihydro-2,7,9a-triazabenzo(*14*)azulen-6(7H)-one ([^{125}I]KX-1) was synthesized as previously described.(*14*) Briefly, KX-01-191 (~100 µg) was dissolved in methanol (50 µl), then iodine-125(^{125}I) radionuclide(Perkin Elmer) in NaOH aqueous (7.83 mCi) was added followed by the addition of a mixture of H_2O_2 (30%) and acetic acid (1:3, 100 µl). The mixture was heated at 100 °C for 30 min. Next, the reaction was quenched with H_2O (4.5 ml) and was purified using an Agilent 1200 series high-performance liquid chromatography system equipped with a C-18 Phenomenex semi-prep column. The product was eluted with acetonitrile and ammonium formate buffer (0.1 M, pH 4.5) (40:60), at a retention time of 11 min. The fraction collected was further diluted with H_2O to a volume of 50 ml. This step was necessary to remove any acetonitrile before biological studies. Finally, the product was then concentrated by first trapping on a C-18 SepPak cartridge (Waters), then [^{125}I]KX1 was eluted with 200 proof ethanol. The average radiochemical recovery yield was 70% and a typical yield ranged from 2-6 mCi of radiolabeled product. The radiochemical and chemical purity of the product was >95%. [^{125}I]KX1 was stable in 200 proof EtOH for at least 30 days with no signs of deiodination.

[^{18}F]FTT was synthesized using the AllinOne (TRASIS, Belgium) fully automated chemistry module as previously described.(*43*) Briefly, 1 mL of a solution containing 7 mg of cryptand and 2 mg potassium carbonate was used to elute $^{18}F/F^-$ from an ion exchange QMA cartridge. The resulting solution was then azeotropically dried with acetonitrile at 100 °C. Next, 0.8-1.0 mg of tosylate-FTT precursor dissolved in DMF was added to the reaction vessel and was heated at 105 °C for 10 min. The reaction mixture was then purified by semi-preparative HPLC using a 40:60 methanol:water mobile phase and [^{18}F]FTT was isolated. The product peak was then diluted with water to reduce the

methanol concentration to <10% and was trapped on a C-18 Sep-Pak (Waters, Waltham MA). The Sep-Pak was then rinsed with 10 mL of water to remove residual methanol solvent and eluted in 1 mL of 200 proof ethanol. Radiosynthesis was done in accordance with current Good Manufacturing Practices (cGMP) for PET radiopharmaceuticals.

[^{125}I]KX1 radioligand binding studies

Using multiple cell lines (table s1), including those engineered in this study, we performed radioligand binding assays in live cells to measure PARP-1 expression through pharmacological saturation assays. Briefly, 50,000 cells/well were plated in 96 well plates 24 hrs before experiments were carried out. On the day of the study, the media from the adherent cells was aspirated and increasing concentrations (0.01 – 10 nM) of [^{125}I]KX1 were added to wells in quadruplicate. Non-specific binding was determined using 10 μM olaparib which saturates all PARP-1 binding sites so any binding observed could be attributed to non-specific sites. Radioligand solutions were allowed to equilibrate on cells for 1 hr at which time wells were washed and then counted on a Perkin Elmer Wizard gamma counter. Control wells were used for protein quantification by the Lowry method. Data was plotted using a non-linear one-site binding hyperbola, and dissociation constant (K_d) and maximum number of binding sites (B_{max}) were generated using Prism Version 6.0.

PARP Inhibitor Growth Inhibition Assays

Cell lines were seeded at a density of 1,000 cells/well in 96 well plates with black coated walls 24 hrs before treatment. Cells were then treated with concentrations varying from 0.02 pM – 100 μM for 7 days. Cell viability was assayed using Cell-Titer Glo (Promega, Madison WI), a chemiluminescent assay that measures ATP and where ATP driven luminescence is relative to cell number. Dose response curves were fitted using Prism version 6.0 and effective concentrations for 50% reduction in cell growth (EC_{50}) were calculated as previously described.

Pre-clinical microPET imaging of PARPi pharmacodynamics

Two orthotopic patient-derived xenograft models were used for pre-clinical imaging including a *BRCA1* mutant (n=1, WO-2-02) and a *BRCA1* WT high PARP-1 expressing tumor (n=3, WO-12-02). The methodology for preparing the orthotopic models has recently been described in the literature.(*40*) Tumors were orthtopically sutured on the ovary of 12 week old female NOD SCID mice purchased from Charles River, Wilmington MA. Animals were first imaged at baseline and then treated later that same day with 50 mg/kg, and then every day including the morning of the second microPET imaging study for a total of 4 doses.

For imaging studies, anesthesia of tumor-bearing mice was maintained via a nose cone at 2-3% isoflurane, 1 L/min oxygen and body temperature was maintained by a heating pad placed under the animal. The mice were injected with 150-300 μCi of [^{18}F]FTT and scanned for 20 minutes from 40-60 minutes post radiotracer administration on a Philips Mosaic HP small animal PET scanner. Images were reconstructed by using 3D-RAMLA protocol with decay correction turned on and normalization set for efficiency. The matrix size was 0.5 x 0.5 x 0.5 mm^3 and field of view was 12.8 cm. Volumes of interest were delineated manually over the tumors, as well as left thigh muscle (reference region), and were consistent with the anatomical location of the tumors. The peak tumor-to-muscle ratio was calculated by maximal counts normalized to percentage of injection dose (%ID/cm^3) from tumor divided by average %ID/cm^3 from reference region. MicroPET images were statistically analyzed using a parametric paired t-test (Prism version 6.0, Graph Pad). After imaging studies with olaparib blocking, ex-vivo autoradiography was performed on the tumor and muscle of mice. Additional control mice (n=3) were used for ex-vivo autoradiography to represent the baseline imaging group. Ex-vivo autoradiography was statistically analyzed using a parametric unpaired t-test (Prism version 6.0, GraphPad).

Tissue handling, storage, and sectioning

Patient tissue samples were handled according to the IRB protocol. Tissue was retrieved at surgery or biopsy and then frozen fresh in OCT embedding media. Tissue sections were produced at 5 μm for either colormetric immunohistochemsity (c-IHC), fluorescent-IHC (f-IHC), or 20 μm for *in vitro* [^{125}I]KX1 autoradiography. Tissue sections were stored at -80 ˚C until used. These methods were chosen to preserve tissue for autoradiography studies that are dependent on PARP-1 enzymatic activity, which is greatly reduced, if not abolished, by standard tissue fixation methods.

Immunohistochemistry and pathologist scoring of PARP-1

Fresh tissue was fixed prior to immunohistochemistry in 10% NBF for 30 min. Next, c-IHC was performed on formalin fixed tissue using antibodies against human keratin marker AE1/3 (Novocastra TM Mouse Monoclonal Antibody, clone AE1/AE3), pan immune cell marker CD45 (Dako M0701, clone LCA), γH2AX (abcam ab22551, Clone 3F2), tumor suppressor p53 (Dako M7001, clone DO-7), and PARP1 (cell signaling 9532, clone 46D11). Staining was done on a Leica Bond-IIITM instrument using the Bond Polymer Refine Detection System (Leica Microsystems DS9800). Heat-induced epitope retrieval was done for 20 minutes with ER2 solution (Leica Microsystems AR9640). Incubation with antibodies was performed at dilutions of: AE1/3 1:400, CD45 1:250, γH2AX 1:400, p53 at 1:60, and PARP1 at 1:100, for 15 min. Next, an 8 min post-primary step and 8 min incubation with polymer HRP were carried out. Finally, endogenous peroxidases were blocked for 5 min followed by the incubation of diaminobenzidine (DAB) for 10 minutes.

PARP-1 staining was scored qualitatively and quantitatively by a clinical pathologist. Quantitative PARP-1 staining was considered positive if greater than 5% of the tumor cells showed nuclear positivity. The intensity of staining was divided into three categories: strong, intermediate and weak.

Fluorescent-immunohistochemistry on clinical tissue

PARP-1 f-IHC was performed using the same antibody as listed above for c-IHC on adjacent tumor sections from clinical samples. Tissue was post-fixed using 4% PFA for 10 minutes, followed by permeabilization with 0.5% Triton-X. PARP-1 staining was performed at 1:1000 dilutions and incubated at room temperature for 1 hr. After primary antibody incubations sections were washed 3 times in 0.2 % PBS with tween 20. Secondary antibodies at 1:200 dilutions were incubated at room temperature for 1 hr then washed as previously described. Slides were counter stained with DAPI and imaged with a 20x objective lens on a Zeiss AxioObserver Z1 microscope (Carl Zeiss Microscopy, LLC, Thornwood, NY, USA). PARP-1 expression was quantified using the co-localization feature of Zeiss Zen software to determine nuclear PARP-1 fluorescent intensity using DAPI to mark the nucleus boundary. The average intensity of four quadrants per section was used for the linear correlation between f-IHC and autoradiography.

Whole section f-IHC was performed using procedures identical to the above except, secondary antibodies with wavelengths of 690 and 800 nm were used and sections were read on a LiCor(Lincoln, Nebraska) fluorescent imager. Regions of interest were drawn in four distinct portions of the tissue and quantified with background subtraction.

Autoradiography on clinical tissue

Fresh frozen tissue sections (20 µm thick) were used for *in vitro* autoradiography with both radiotracers [^{125}I]KX1. Autoradiography was performed on all patient sections in the same experiment to produce relative data between patient samples. Sections were removed from the – 80 ˚C storage and equilibrated to room temperature for 5 minutes following rehydration in PBS for 3 minutes. Next, radiotracers were incubated on sections at a single concentration in the range of 5-10 nM and were allowed to equilibrate at room temperature for 45 minutes. These radiotracer concentrations were chosen due to previous studies where we have shown that these concentrations are high enough to saturate PARP-1 *in vitro*. Sections were washed 3 times at 3 minutes/wash and slides were dried

then exposed to a phosphorimager film for 24 hrs. Plates were read on a Perkin Elmer digital phosphorimager and max intensity for regions of interest were generated using Perkin Elmer Image Quant software. Iodine-125 standards (American Radiolabeled Chemicals) were used to generate standard curves to measure the linearity of the activity range on the system and convert final values to μCi/mg (or 37 kbq/mg) units. Max intensity was used as the quantitative measurement that was applied in correlative studies between f-IHC and PET imaging.

Clinical [^{18}F]FTT PET imaging and histological correlates

Patients that underwent [^{18}F]FTT PET/CT imaging followed by surgical biopsy or debulking were included in a correlation analysis between radiotracer uptake ([^{18}F]FTT and FDG) and *in vitro* markers of PARP-1 expression (PARP-1 f-IHC and [^{125}I]KX1). Patients that did not undergo [^{18}F]FTT PET imaging, but had tissue samples were included in correlation analysis of in vitro tissue markers. Correlations were performed using a linear-regression model and Pearson correlation coefficient (Prism version 6.0, GraphPad).

Study Design

This was a phase I pilot study using the novel radiotracer [^{18}F]FluorThanatrace ([^{18}F]FTT). Patients with known or suspected epithelial ovarian, fallopian tube, or primary peritoneal cancer were eligible for this study. Patients were allowed to participate in this study if they are at least 18 years of age. Volunteers that meet the eligibility criteria were considered for study participation regardless of race or ethnic background. We anticipated enrolling up to 30 evaluable subjects who meet eligibility requirements for this study. Due to the nature of the disease population all subjects were women. Accrual occurred over approximately 1.5 years.

Positron emission tomography (PET/CT) imaging was used to evaluate biodistribution and *in vivo* PARP-1 activity in sites of active tumor using the investigational radiotracer [^{18}F]FTT. Each patient received approximately 10 mCi (370 MBq) of [^{18}F]FTT intravenously (approximated range for

most studies was 8-12 mCi or 296-444 MBq). The study included two different cohorts of subjects - a biodistribution cohort and a dynamic cohort - with a different imaging protocol for each group. The patients presented in this study with correlative tissue were all enrolled in the dynamic cohort. The patient presented in s6 was in the biodistribution cohort and was used as an example where inter-tumor heterogeneity was evident on [^{18}F]FTT PET/CT. The Dynamic cohort underwent approximately 60 minutes of dynamic imaging over the abdomen/pelvis (or field-of-view that includes known tumor) followed by up to 2 static skull base to mid-thigh scans done at approximately 90 and approximately 180 minutes after injection of [^{18}F]FTT. The static scans were optional at the discretion of the investigator or study physician. The imaging data was used to collect preliminary data on PARP-1 uptake in tumor using the investigational radiotracer [^{18}F]FTT and was compared to pathology assays, when available. Imaging was performed using a whole-body PET/CT scanner (Philips Medical Systems, Netherland). The protocol was performed under the regulatory approval of the IRB and IND.

Inclusion Criteria for Dynamic cohort

Participants were ≥ 18 years of age with history of known or suspected epithelial ovarian, fallopian tube, or primary peritoneal cancer (may have primary or recurrent cancer at the time of study enrollment). At least one lesion ≥ 1.0 cm that is seen on standard imaging (e.g. CT, MRI, ultrasound, FDG PET/CT). Were willing to consent to collection of pathology tissue for the purposes of research at the time of clinical biopsy or surgical procedure (tissue was only collected if procedure is planned as part of clinical care or if tumor is readily accessible for biopsy, and was sometimes obtained for research purposes only).

Exclusion Criteria for Dynamic cohort

Females who were pregnant or breast feeding at the time of screening were not eligible for this study; a urine pregnancy test was performed in women of child-bearing potential at screening. Inability to

tolerate imaging procedures in the opinion of an investigator or treating physician. Any medical condition, illness, or disorder as assessed by medical record review and/or self-reported that was considered by a physician investigator to be a condition that could compromise participant safety or successful participation in the study. Only individuals (aged 18 or over) who can understand and give informed consent will be eligible to participate in this study. Individuals who were considered to be mentally disabled were not be recruited for this study. All subjects must have understood and been able to give informed consent. This should negate any undue influence or coercion.

[^{18}F]FTT PET/CT Image Analysis

The overall quality of the generated images was evaluated. Initial imaging of the skull base to mid-thigh was used to investigate regional tracer uptake in tumor and normal tissues for this novel radio tracer. Uptake in specific tumor sites was analyzed both qualitatively and quantitatively to evaluate the activity of this radiotracer in humans. Uptake and retention of [^{18}F]FTT in known sites of tumor was evaluated visually by trained radiology readers, the principal investigator or designee.

Supplemental Tables

Table s1: Cell lines produced or used in this study.

Cell line	BRCA status	Modified genes	Acquired from
UWB1.289	*BRCA1* mutant exon11 625delAG	None	ATCC
UWB1.289-*BRCA1*^{restored}	*BRCA1* cDNA insertion	*BRCA1* restored	ATCC
UWB1.289-*PARP1* KO G1	*BRCA1* mutant exon11 625delAG	*PARP1* KO Stable Cas9 expression	This work
UWB1.289-*PARP1* KO G2	*BRCA1* mutant exon11 625delAG	*PARP1* KO Stable Cas9 expression	This work
UWB1.289-*PARP1* KO G3	*BRCA1* mutant exon11 625delAG	*PARP1* KO Stable Cas9 expression	This work
OVCAR8	*BRCA1* promoter methylation	None	David M. Livingston, Dan Farber Cancer Institute
OVCAR8-*PARP1* KO G1	*BRCA1* promoter methylation	*PARP1* KO Stable Cas9 expression	This work
OVCAR8-*PARP1* KO G2	*BRCA1* promoter methylation	*PARP1* KO Stable Cas9 expression	This work
OVCAR8-*PARP1* KO G3	*BRCA1* promoter methylation	*PARP1* KO Stable Cas9 expression	This work
SNU-251	*BRCA1* mutant exon 23 W1815X (5564G > A)	None	Basser Center for BRCA
PEO4	*BRCA2* reversion mutation Primary mutation [5193C>G (Y1655Y)] Secondary mutation [5193C>T (Y1655Y)]	None	ATCC
SKOV3	WT	None	ATCC

Table s2: [^{125}I]KX1 radioligand binding results from PARP-1 saturation assays.

Cell line	Kd(nM)	SEM	Bmax(fmol/mg)	SEM
UWB1.289	3.0	0.01	9204	14.4
UWB1.289-BRCA1^{restored}	2.1	0.03	5910	31.4
UWB1.289-PARP1 KO-G1	1.7	0.07	1626	24.1
UWB1.289-PARP1 KO-G2	1.7	0.05	1716	17.3
UWB1.289-PARP1 KO-G3	1.8	0.14	1410	38.9
OVCAR8	4.2	0.06	5666	40.8
OVCAR8-PARP1 KO-G1	1.5	0.11	619.7	15.7
OVCAR8-PARP1 KO-G2	2.3	0.25	965.8	40.2
OVCAR8-PARP1 KO-G3	1.9	0.18	855.5	28.7
SNU-251	0.6	0.05	4268	99.6
SKOV3	2.2	0.04	3139	19.6
PEO4	0.7	0.02	2397	16.0

K_d dissociation constant

B_{max} maximum number of PARP-1 binding sites

SEM standard error of measurement

Table s3a: *In vitro* effective concentrations for 50% reduction in viability of cell lines treated with PARPi.

Cell line	Talazoparib		Niraparib		Rucaparib	
UWB1.289	-5.13	0.21	-1.64	0.04	-1.71	0.09
UWB1.289-BRCA1	-3.78	0.34	-0.57	0.07	-0.04	0.06
UWB1.289 PARP1 KO G3	-0.73	0.08	-0.03	0.06	-0.02	0.06
UWB1.289 PARP1 KO G2	-0.82	0.09	-0.12	0.07	-0.16	0.07
UWB1.289 PARP1 KO G1	-0.24	0.08	0.24	0.05	0.24	0.06
OVCAR8	-3.14	0.22	-1.01	0.04	-0.37	0.05
OVCAR8 PARP1 KO G1	0.50	0.09	0.43	0.08	0.49	0.08
OVCAR8 PARP1 KO G2	0.39	0.09	0.37	0.08	0.41	0.06
OVCAR8 PARP1 KO G3	0.51	0.07	0.41	0.06	0.48	0.05
SNU-251	-4.69	0.34	-0.23	0.08	-1.40	0.13
SKOV3	-0.70	0.04	-0.05	0.04	0.69	0.02
PEO4	-0.60	0.10	0.40	0.08	0.36	0.06

Table s3b: *In vitro* effective concentrations for 50% reduction in viability of cell lines treated with PARPi.

Cell line	Olaparib		Veliparib		Cisplatin	
UWB1.289	-0.68	0.08	-0.02	0.07	-1.33	0.04
UWB1.289-BRCA1	0.55	0.06	1.09	0.04	-1.12	0.03
UWB1.289 PARP1 KO G3	0.48	0.07	1.28	0.06	-0.94	0.05
UWB1.289 PARP1 KO G2	0.34	0.09	1.18	0.09	-0.93	0.06
UWB1.289 PARP1 KO G1	0.73	0.07	1.38	0.06	-0.74	0.05
OVCAR8	0.01	0.04	0.78	0.06	-0.14	0.04
OVCAR8 PARP1 KO G1	1.24	0.12	1.53	0.11	-0.23	0.06
OVCAR8 PARP1 KO G2	1.09	0.11	1.53	0.09	-0.27	0.05
OVCAR8 PARP1 KO G3	1.18	0.08	1.52	0.08	-0.27	0.04
SNU-251	0.20	0.04	0.98	0.06	-0.46	0.05
SKOV3	0.93	0.03	1.68	0.02	0.51	0.03
PEO4	0.68	0.09	1.65	0.07	0.17	0.05

- Data presented as $EC_{50,}$ SEM for each drug in log μM concentrations
- EC_{50} is the effective concentration to reduce cell viability by 50% compared to healthy controls

Table s4: Biomarker analysis.

Biomarker	**AE1/3**	**LCA**	**p53**	**PARP-1**	**γH2AX**
total(%)	12(92)	8(62)	10(77)	13(100)	13(100)

Table s5: Uptake on PET/CT imaging and autoradiography correlates.

			PET/CT		Histological correlates	
Pt #	**Tissue Site**	**Cancer Yes or No**	**[^{18}F]FTT SUVmax**	**[^{18}F]FDG SUVmax**	**[^{126}I]KX1 autoradiog-raphy µCi/mg max**	**PARP-1 immunoflu-orescence RFU**
2	ovary	Yes	5.4	4.1	0.12	42.7
2	omentum1	Yes	7.8	3.4	0.20	50.7
2	RLQ lesion	Yes	5.1	2.0		
4	ovary	No	2.3	2.5	0.01	24.2
4	ovary	Yes	5.5	11.6	0.16	40.1
7	vaginal	Yes	12.1	8.5	0.28	59.2
9	ovary	Yes	4.1	10.6	0.01	26.8
11	omentum	Yes	2.4	3.7	0.05	39.3
11	ovary	Yes	2.3	2.9	0.03	25.4
12	rectal mass	Yes	5.7	13.9	0.05	22.2
13	ovary	Yes	2.6	11.2	0.09	34.3
14	ovary*	Yes	No scan		0.41	50.3
16	lymph node*	Yes^	NV	NV	0.23	47.9
17	ovary*	Yes	No scan		0.75	71.8

* [^{18}F]FTT PET imaging was not performed due to immediate surgical treatment

RFU relative fluorescent units

NV not visualized on PET with [^{18}F]FTT or [^{18}F]FDG

^ 10 – 20 tumor cells located on pathological analysis

Table s6: Patient characteristics.

Pt#	Age	Histology	Prior Treatments	Stage	Disease Status	BRCA	Platinum Sensitivity	Past Regimens
2	63	HGSOC[α]	Carboplatin/ paclitaxel x3 (NAT)[β]	IIIC	2	Wt	N/A	1
4	48	Seromucinous carcinoma, grade 1	None	IIA	3	Wt	yes	0
7	63	HGSOC[α]	None		2	Wt	yes	2
9	22	Borderline serous	None	IIIA2	3	Unknown	N/A	0
11	60	Poorly differentiated carcinoma	Carboplatin/ paclitaxel x3 (NAT)[β]	IIIC	1	*BRCA2*	Yes	0
12	67	HGSOC[α]	Rucaparib x 2 years	IIIC	2	*BRCA1*	Yes	3
13	34	Borderline serous	None	IC	3	Unknown	N/A	0
14*	42	HGSOC[α]	Carboplatin/ paclitaxel	IIIC	N/A	*BRCA1*	Yes	N/A
16	41	HGSOC[α]	Carboplatin/ paclitaxel x3 (NAT) [β]	IVb	1	*BRCA1*, VUS	N/A	0
17*	68	HGSOC[α]	None	IIIc	N/A	Unknown	N/A	0

*No scan

[α]HGSOC: high grade serous ovarian carcinoma

[β]NAT: neoadjuvant chemotherapy

VUS: variant of uncertain significance

Supplemental Figures

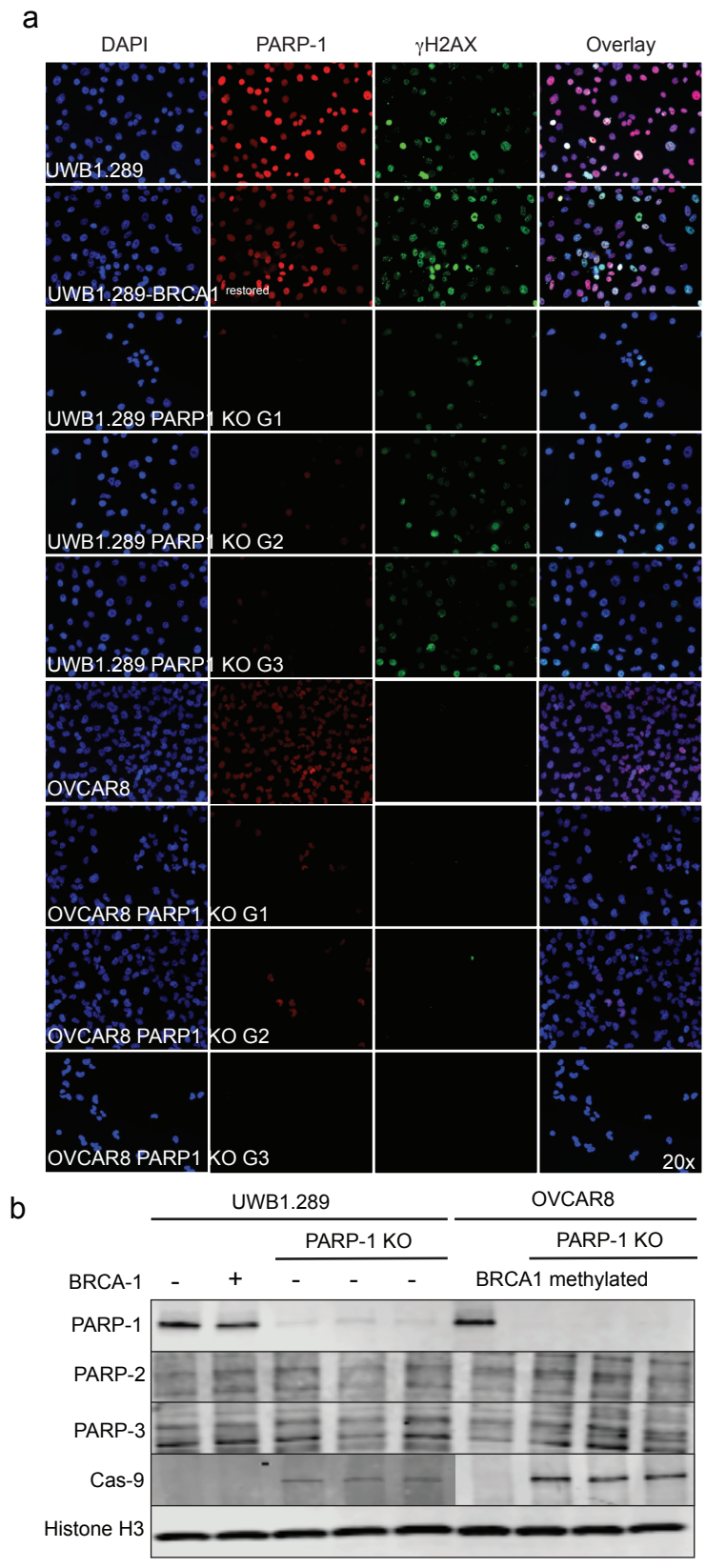

Figure s1: In vitro characterization of *PARP1* KO cell lines used. **A)** Cell microscopy showed significant reductions in PARP-1 expression in *PARP1* KO cell lines at the single cell level. The majority of clones in the polyclonal population had no PARP-1 expression compared to parent controls. Cropped images showing single cells are also shown in figure 1a. **B)** Western blot analysis of polyclonal populations of *PARP1* KO cell lines showed >90% reduction in PARP-1, with no effect observed for PARP-2 or PARP-3 from parent control. Cas9 expression was confirmed in transfected cell lines. PARP-1 and Histone-H3 Western blots reshown from figure 1b.

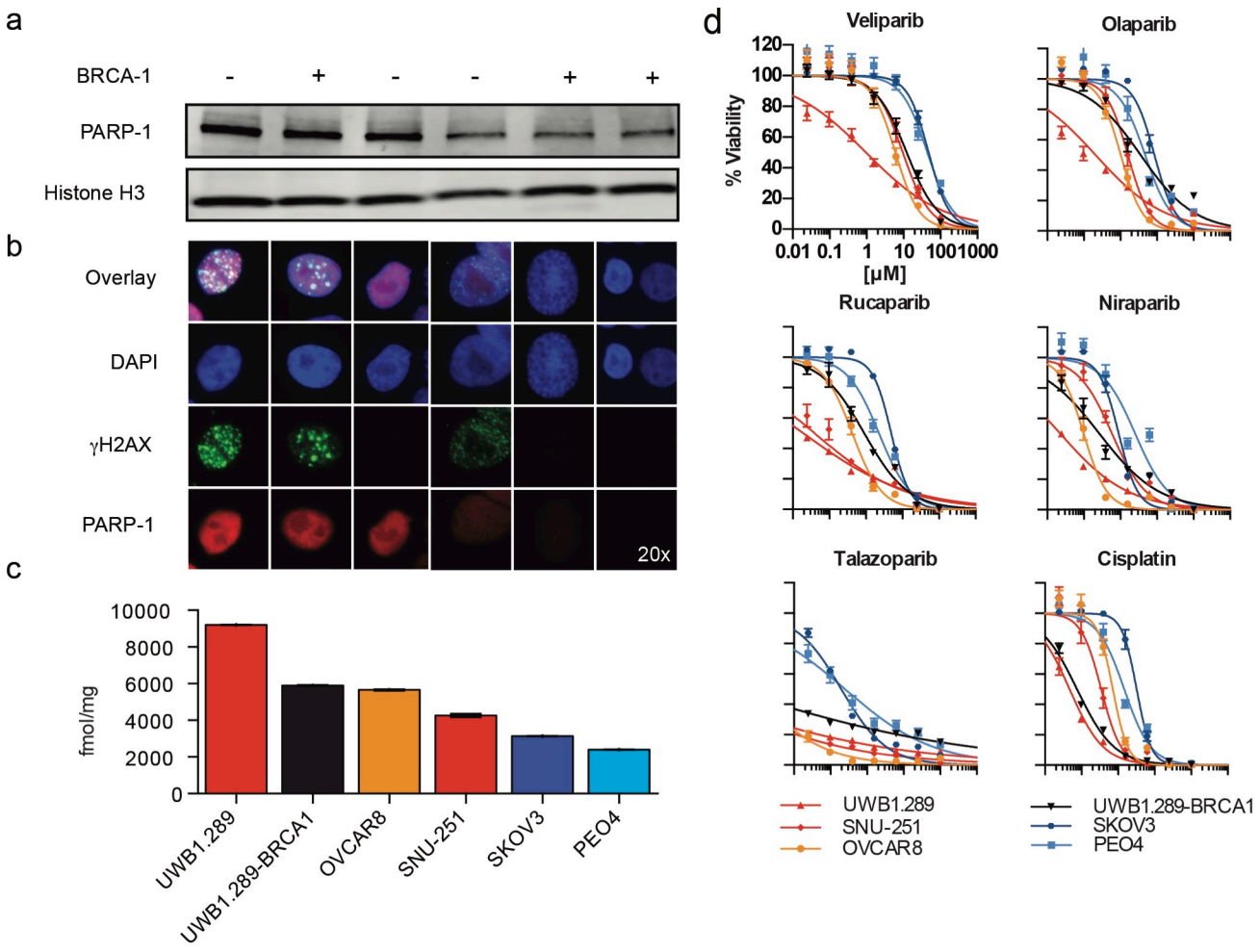

Figure s2: Comparing PARP-1 expression in ovarian cancer cell lines and their sensitivity to PARPi. Refer to table s1 for cell line characteristics regarding BRCA status. **A)** Using Western blot analysis we showed that there is a spectrum of PARP-1 expression in ovarian cancer cell lines. **B)** Cell microscopy showed similar results to Western blot and this data. Cell microscopy images of UWB1.289, UWB1.289-BRCA1, and OVCAR8 are reshown from figure 1a. **C)** [^{125}I]KX1 radiotracer uptake corresponded to PARP-1 expression. **D)** In vitro cell viability data showed differential sensitivities to PARPi with SKOV3 and PEO4 cell lines showing the lowest sensitivity.

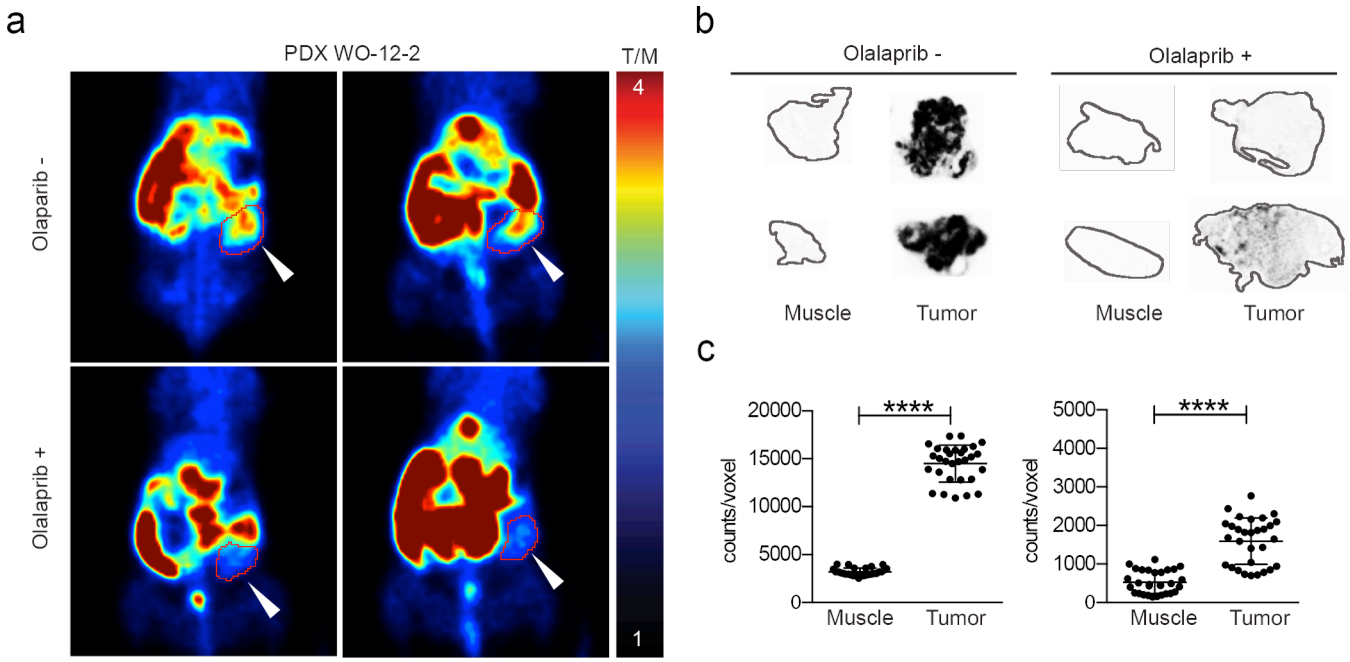

Figure s3: [^{18}F]FTT microPET images shown with *ex vivo* autoradiographs. **A)** [^{18}F]FTT microPET images of a patient derived xenograft model of an ovarian carcinoma (*BRCA1* WT*) before and after treatment with olaparib. **B)** Ex vivo autoradiography was performed side by side to confirm microPET imaging results. Olaparib untreated (-) tumors showed higher radiotracer signal compared to olaparib treated (+) groups in autoradiographs (n=4). **C)** Ex-vivo autoradiography of muscle and tumor for olaparib untreated (-) and olaparib treated (+) groups show statistically significant differences for both groups (n=4, 10 sections/tumor or muscle, parametric unpaired t-test, p-values < 0.0001).

*WT – wild type

A)

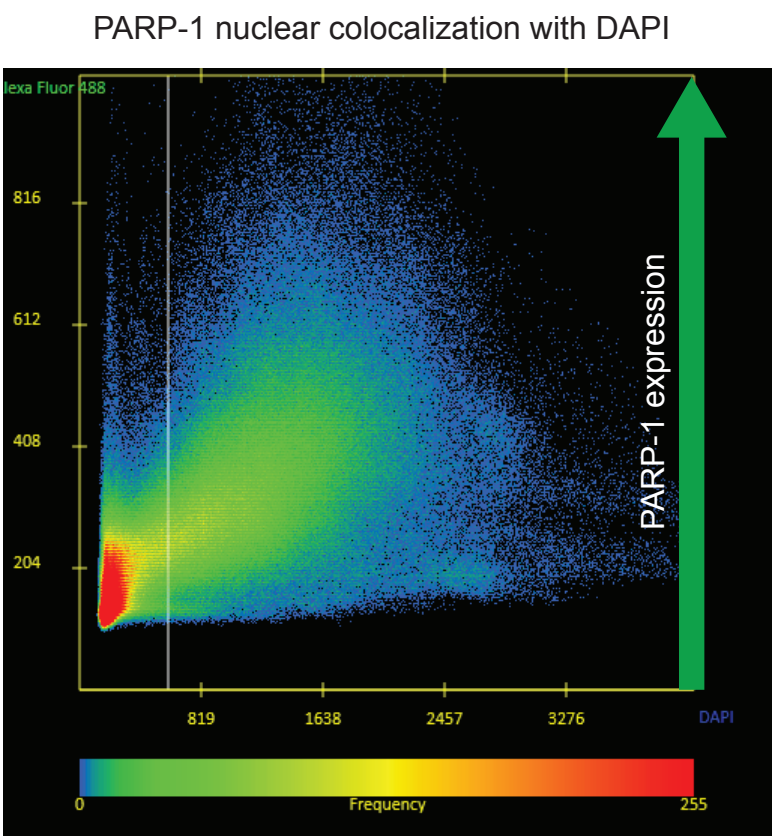

B)

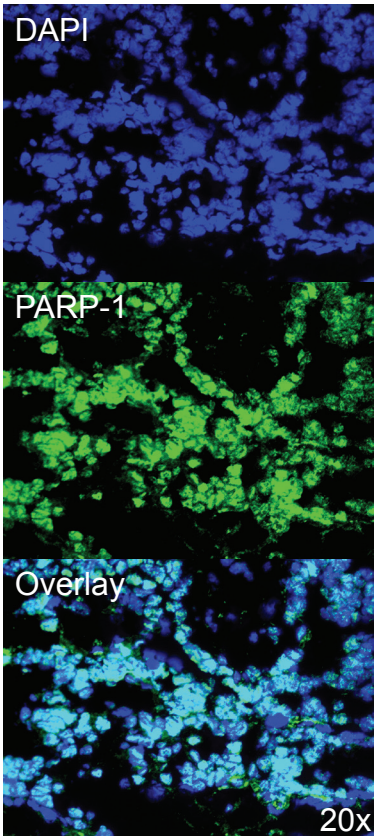

Figure s4: Fluorescent immunohistochemistry (f-IHC) was analyzed using Zeiss Zen software and a nuclear co-localization method that quantified PARP-1 fluorescent intensity that co-localized with nuclear marker DAPI. **A)** Here we show a representative co-localization scatter plot and **B)** representative images of tissue stained for DAPI (top), PARP-1 (middle), and the overlay (bottom).

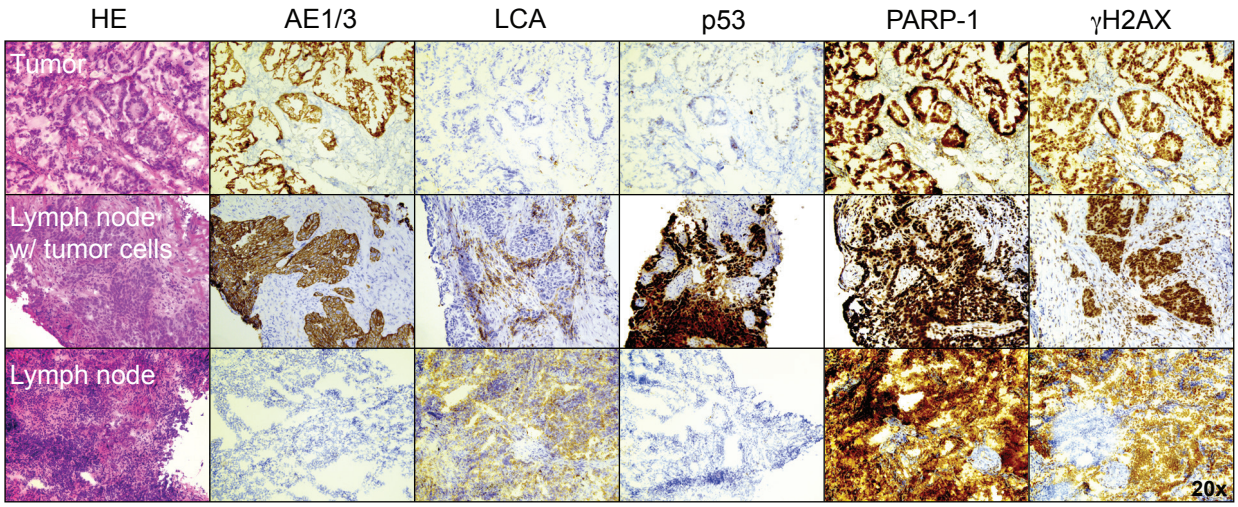

Figure s5: Immunohistochemistry on adjacent tissue sections for biomarkers including AE1/3*, LCA**, p53, γH2AX, and PARP-1. Shown are three representative cases which highlight the presence of PARP-1 in both primary tumor and lymph nodes with or without nodal disease. Strong PARP-1 and γH2AX staining was observed in both tumor and non-tumor tissue in all samples irrespective of p53.

AE1/3* – keratin marker commonly used to identify ovarian cancer cells

LCA** – pan lymphocyte marker

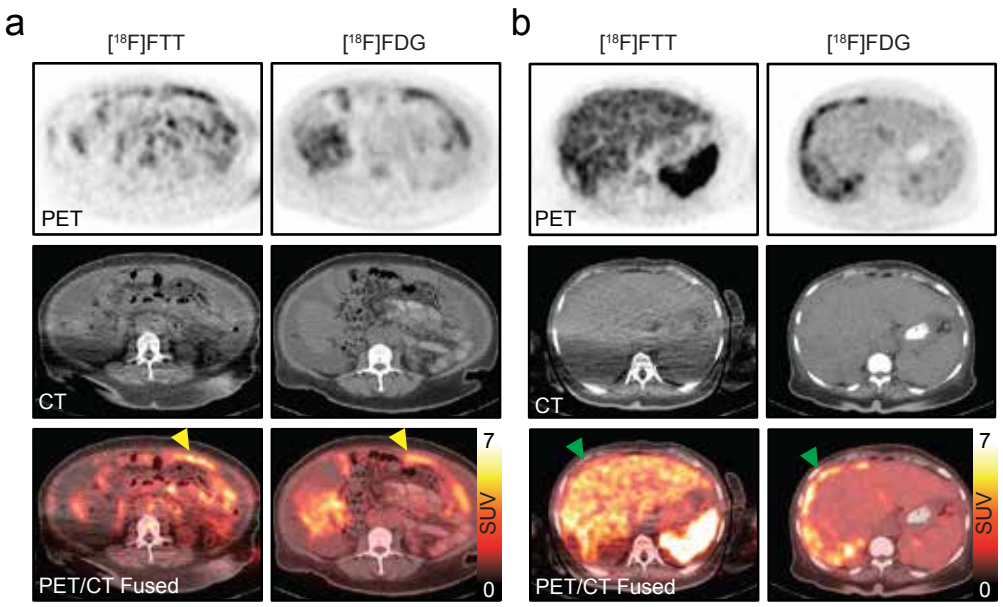

Figure s6: Heterogeneity of [^{18}F]FTT uptake between lesions in the same patient: PET images demonstrate omental disease in the left abdomen which demonstrates uptake on both [^{18}F]FTT and [^{18}F]FDG (yellow arrows: [^{18}F]FTT SUV_{MAX} = 6.9, [^{18}F]FDG SUV_{MAX} = 5.4). Carcinomatous hepatic implants demonstrate uptake on [^{18}F]FDG (green arrow: [^{18}F]FDG SUV_{MAX} = 6.7), but on [^{18}F]FTT demonstrate uptake less than that of liver (mean liver SUV = 4.4). This patient was in the dosimetry cohort; the above [^{18}F]FTT images were obtained at approximately 2 hours after radiotracer injection.